The effect of waves on engine-propeller dynamics and propulsion performance of ships

Bhushan Taskar[a], Kevin Koosup Yum[a], Sverre Steen[a], Eilif Pedersen[a]

[a] Department of Marine Technology, Norwegian University of Science and Technology (NTNU), Trondheim, Norway

Corresponding Author: Bhushan Taskar (bhushan.taskar@ntnu.no)

1 Abstract

This paper investigates the effect of waves on the propulsion system of a ship. In order to study the propulsion in different wave conditions, a procedure for wake estimation in waves has been implemented. A clear drop in the propulsion performance was observed in waves when engine propeller dynamics, wake variation and thrust and torque losses were taken into account. This can explain the drop in vessel performance often experienced in presence of waves in addition to the effect of added resistance. Therefore, performance prediction of ships in rough weather can be improved if the effects of waves on the propulsion system are considered. Specific problems causing drop in performance have also been identified. System response in case of extreme events like propeller emergence has been simulated for analyzing the performance and safety of the propulsion system. The framework of engine-propeller coupling demonstrated in this paper can also be used to analyze different components of propulsion system (e.g. propeller shaft, control system) in higher detail with realistic inputs. This paper is a step towards optimizing the propulsion of ships for realistic operating conditions rather than calm water condition for energy efficient and economic ships.

Keywords: Propulsion in waves, Engine Propeller Dynamics, Propulsion Performance, Propulsion Losses in Waves, Marine Propellers, Engine control in waves.

Preprint submitted to Ocean Engineering
DOI: 10.1016/j.oceaneng.2016.06.034

2 List of variables

h	Depth of the propeller shaft
R	Propeller radius
β	Thrust diminution factor
w_P	Effective wake fraction
U	Ship speed
A	Wave amplitude (m)
λ	Wavelength
L	Ship length
ω_e	Wave encounter circular frequency
ξ_a	Surge amplitude with phase delay of ζ_ξ
ζ_ξ	Phase delay
ω	Wave circular frequency
h_a	Wave amplitude
k	Wave number
$(x_P, 0, z_P)$	Propeller co-ordinates
t	Time
X	Wave encounter angle (0 for following sea; 180 for head sea)
α	Coefficient representing effect of wave amplitude decrease at the stern

DOI: 10.1016/j.oceaneng.2016.06.034

$V_{fluctuating}$	Wake velocity considering fluctuations due to waves
V_{mean}	New wake velocity considering the effect of pitching motion
V_{total}	Total wake velocity considering mean increase as well as wake fluctuations
x	Longitudinal distance of the propeller from the center of gravity of the ship
$\Delta\bar{p}$	Pressure gradient below the bottom of the ship due to pitching motion
η_5	Pitch amplitude
m	Mass of ship
m'	Surge added mass of ship
$\ddot{x}$	Surge acceleration of ship
$\dot{x}$	Surge speed of ship
T'	Thrust produced by the propeller
t'	Thrust deduction fraction
ρ	Density of seawater
S	Wetted surface area of the ship
C_T	Total resistance coefficient of the ship
R_1	Added resistance of the ship in waves
J_{Shaft}	Mass moment of inertia of the propeller shaft
ω_{Shaft}	Propeller shaft speed
a_1	Friction coefficient for the main engine

DOI: 10.1016/j.oceaneng.2016.06.034

a_2	Friction coefficient of the propulsion shaft
Q_{Eng}	Engine torque
Q_{Load}	Propeller load torque
η_m	Mechanical efficiency of engine crank system
p	Pressure
T	Temperature
F	Fuel-air equivalent ratio
M	Mass of gas
$\dot{M}$	Mass flow of gas or rate of change of mass in a control volume
M_b	Mass of burned fuel in gas
$\dot{M}_b$	Mass flow or rate of change of mass of burned fuel in gas
E	Energy in a volume
$\dot{E}$	Energy flow or rate of change in energy in a control volume
V	Volume
$\dot{V}$	Rate of change of volume

Abbreviations

MCR	Maximum continuous rating
BSFC	Brake specific fuel consumption
EVC	Exhaust valve close

DOI: 10.1016/j.oceaneng.2016.06.034

3 Introduction

Traditionally, ships have been optimized for calm water operation, because this is the intended condition during the contractual sea trials, and probably also because one has not had the knowledge and tools to optimize ships properly for operations in waves. Ships have of course been designed to be safe in all operational conditions they are supposed to be used in, but not to be optimally efficient in the typical operation condition, which for most ships is not calm water. Optimization for operation in waves is increasingly viable, and so it is expected that more energy-efficient and economical ships can be designed if seakeeping and powering in waves is taken into account in the design optimization.

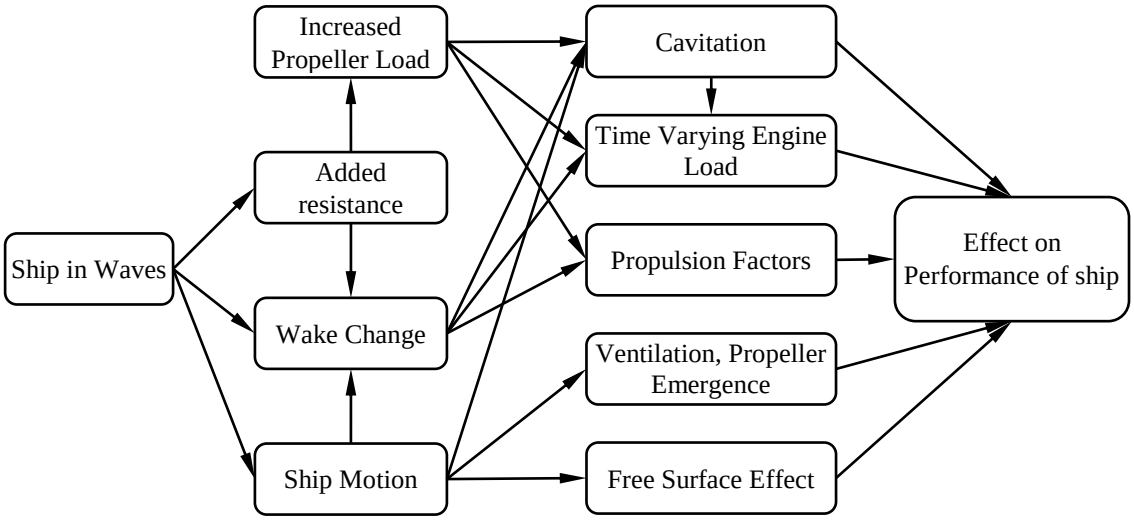

Figure 1 The effects of waves on ship propulsion

Currently, propulsion plants are optimized for calm water operation. While off-design conditions like rough weather are taken care of by adding simple sea margin to the required power. Sea margin is typically 15 to 25% of the power required in calm water condition. However, to optimize the installed engine size, sea margin should be accurately calculated based on the performance of ship in worst intended operating condition, so that minimum possible engine power can be used while still ensuring safety and performance of vessel. Various factors affecting the ship performance in waves can be seen in Figure 1.

DOI: 10.1016/j.oceaneng.2016.06.034

The effects of waves on the propulsion system are yet to be clearly understood. It has been observed that the system of engine and propeller react to the time varying flow field encountered in waves, and it would be useful to simulate this effect, to take into account the effect of waves on the engine propeller system already on the design stage. In case of propeller emergence, when the propeller is coming partly out of the water, the propeller torque drops significantly, and depending on how the engine is controlled, propeller racing might occur. This is one of the primary indicators for voluntary speed reduction. Therefore, to predict attainable speed in waves and engine dynamic response, prediction of propeller emergence is important.

In waves, changes in flow field alters propulsion factors as compared to calm water condition. Nakamura and Naito (1975) have demonstrated the effect of waves and ship motions on thrust deduction and wake fraction of a ship. Wake is also affected by pitching motion of a ship, causing increase in average wake (Faltinsen, Minsaas et al. 1980) along with wake fluctuations (Ueno, Tsukada et al. 2013). Significant changes in wake field were observed in presence of waves and ship motions in the RANS simulations carried out by Guo, Steen et al. (2012), where the nominal wake field was obtained in waves. Similar results were obtained by Sadat-Hosseini, Wu et al. (2013) where wake was obtained in presence of waves using particle image velocimetry (PIV).

Changes in flow field explained previously cause fluctuations in propeller thrust and torque as observed by Nakamura and Naito (1975), Lee (1983) and Amini (2011). Taskar and Steen (2015) have identified a need to study the effect of large torque variations observed in presence of waves on engine performance. Moreover, waves cause surge motions and periodic change in propeller submergence due to heave and pitch. Such changes in propeller submergence, surge motion and occasional propeller emergence give rise to fluctuating loads on the engine. This may affect engine performance as well as propeller performance due to shaft speed variations. Therefore, engine and propeller should be studied together as a system to correctly simulate interaction between them. Also, ship and propeller dynamics

should be taken into account while optimizing the control strategy of machinery (Kyrtatos 1997). Investigations by Taskar, Yum et al. (2015), have shown that unsteady propeller inflow can cause significant increase in power and fuel consumption in order to keep the ship speed constant.

Variable loads on the propeller in presence of waves can cause mechanical failures (Amini 2011). Therefore, it is necessary to estimate the magnitude of such loads. Tanizawa, Kitagawa et al. (2013) have developed a methodology to include realistic engine response in the self-propulsion tests to emulate real condition and get accurate estimates of fuel consumption in waves at different pitch settings in case of controllable pitch propellers. It also serves the purpose of obtaining realistic dynamic response of the ship's propulsion system. Queutey, Wackers et al. (2014) have studied the effect of waves on the flow around a ship with pod, considering the effect of waves on cavitation and ventilation with the help of model tests and experiments. The effect of environmental conditions like wind and waves on the propulsion performance has been studied by Kayano, Yabuki et al. (2013) using full scale experiments. They observed that DHP (Delivered Horse Power) measured in the full-scale experiments in presence of wind and waves was higher than the estimated value and propulsive efficiency lower than the estimated value. Therefore, need of predicting power curve more precisely considering the effect of wind and waves was proposed in order to improve the energy saving of ship operations.

For the study of coupled dynamics of vessel-propulsion-diesel engine system, Kyrtatos, Theodossopoulos et al. (1999) conducted a simulation of propeller – diesel engine dynamics and applied a PI governor. The engine model used was built based on the filling and emptying approach and phenomenological submodels for combustion and scavenging. They demonstrated the model's reliability to test the governor in different transient load. Livanos, Simotas et al. (2006)and Theotokatos and Tzelepis (2013) studied coupled dynamics for a vessel-propulsion-diesel engine system. The first tested the case with a controllable pitch propeller under maneuvering operation with primary interest on the engine system response like shaft speed, turbocharger speed and power development under transient load. The engine

model used was a mean value model, derived from their phenomenological model called MoTher. The latter authors did a similar study with more focus on emission from the engine. Campora and Figari (2003) used a phenomenological engine model with two-zone description in the cylinder for the coupled simulation. Their simulation result was validated by full-scale measurement. In all studies mentioned, the propeller is modelled as either a basic propeller model, obtained from an open water performance test, or as a time series of experimentally measured torques. Therefore, influence of waves on the propulsion system is excluded or statically taken into account.

In this paper, we have investigated effects of waves on the propulsion system. Waves from different directions causing unsteady interaction between engine and propeller have been studied. Events like propeller emergence have been simulated to observe the combined behaviour of engine, response of control system and its effect on the vessel operation. The total efficiency of the propulsion system has been investigated in presence of waves to check if a drop in propulsive efficiency should be taken into account for power and speed predictions in waves. This paper also explores the validity of computing unsteady propeller loads using the assumption of constant propeller speed.

For this investigation, a coupled model of engine and propeller has been implemented in MATLAB-Simulink along with a method to estimate wake in waves. Multiple wave conditions have been simulated with different wavelengths, wave heights and wave directions to observe their impact on the propulsion. This study demonstrates the importance of using a coupled engine propeller system for accurate estimation of ship performance. It can be further used to optimize installed power while ensuring safety of vessel in all weather conditions, rather than just adding a simple sea margin. This study will also clarify the effects of propeller emergence on the engine performance.

Preprint submitted to Ocean Engineering
DOI: 10.1016/j.oceaneng.2016.06.034

4 Geometries and wake data

Wake field is one of the important inputs required for the propeller design and performance estimation. Therefore, to study the effect of waves on propeller performance, it is essential to know the wake field in waves. However, wake data in waves are rarely available since in most of the cases the wake field is obtained only in calm water condition. It is also both complicated and time-consuming to acquire such data. Sadat-Hosseini, Wu et al. (2013) performed model tests on the KVLCC2 hull to obtain wake fields in three different waves. Therefore, KVLCC2 was used as a case vessel for this study. Hull geometric details are found in Table 1. Sadat-Hosseini, Wu et al. (2013) have carried out experiments in head sea conditions using PIV measurements. Nominal wake observations were performed for wavelength to ship length ratios of 0.6, 1.1 and 1.6 at 8, 12 and 6 time instants respectively for each wave period. Their study also reports CFD simulations validated with the PIV measurements. For our analysis, we have used the CFD data because it is smoother and less noisy compared to the PIV measurements. However, CFD data and PIV measurements are available only for head sea condition.

Table 1 Ship particulars

Length beween perpendiculars (m)	320.0
Length at water line (m)	325.5
Breadth at water line (m)	58.0
Depth (m)	30.0
Draft (m)	20.8
Displacement (m^3)	312622
Block Coefficient (C_B)	0.8098
Design Speed (m/s)	7.97

The propeller design was altered in order to match the existing engine model. Pitch of the propeller blades was uniformly changed to be able to deliver maximum engine power. Geometric details of this

DOI: 10.1016/j.oceaneng.2016.06.034

design can be seen in Table 2. There is no engine specified for KVLCC2 by her designers. In this study, an existing engine model was used with fine-tuned parameters and validated against data from the manufacturer of the engine used in this paper. Selection of engine was limited by the availability of the data to validate the simulation model. Since the power of the available engine model was insufficient to propel the hull at design speed, simulations were run at a lower vessel speed, chosen such that the engine runs at 85% MCR (Maximum Continuous Rating). The design speed of KVLCC2 is 15.5 knots, while the simulations were performed for a speed of 14.7 knots.

Table 2 Propeller geometry

Diameter (D) (m)	9.86
No of blades	4
Hub diameter (m)	1.53
Rotational speed (RPM)	95
A_e / A_0	0.431
$(P/D)_{mean}$	0.47
Skew (°)	21.15
Rake (°)	0

4.1 Wake Contraction Procedure

Wake distribution was available in model scale only, and needed to be contracted to obtain ship scale wake. According to the ITTC (2011), the wake scaling procedure given by Sasajima, Tanaka et al. (1966) is most commonly used and gives reasonable results. In this method, frictional wake is obtained by separating the potential wake from the total wake field. Frictional wake is then scaled and added to the potential wake to obtain ship scale wake. However, in absence of potential wake data we have contracted the total wake field by the ratio of viscous resistance coefficient between model and full scale. Hence, the difference between potential wake component of model and ship has been neglected.

Potential wake is almost constant in the propeller plane as seen from the typical ship scale wake presented in ITTC (2011). In such cases, the same full-scale total wake would be obtained by scaling the total wake or just the frictional component of the model-scale wake. The only error would be due to the neglected correction in the potential wake. This procedure has been applied to each snapshot of the wake field at different times as if it were calm water wake distribution. Model and full-scale wakes can be seen in Figure 2.

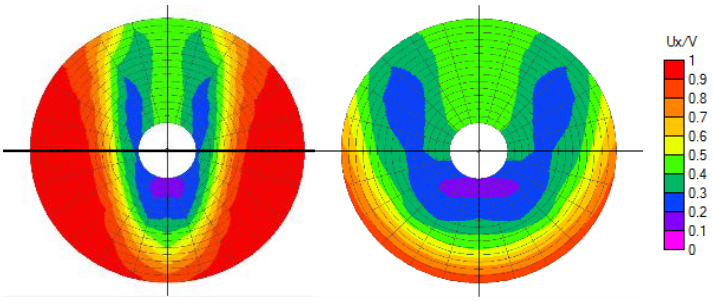

Figure 2 Full scale contracted wake velocities (Left) and model scale wake velocities (Right)

4.2 Ship motion and added resistance calculations

Ship motion RAOs were calculated using linear strip theory, utilizing potential theory and pressure integration, implemented in the ShipX Veres software. Surge, pitch and relative stern motion RAOs have been calculated. Pitch RAO is required to calculate mean increase in propeller inflow using Faltinsen's method (described later). RAO for relative stern motion has been used to compute variation in thrust and torque due to the variation in propeller submergence in different wave conditions. Surge motion RAO is necessary to compute wake fluctuations in waves using Ueno's method (described later). These RAOs can be seen in Figure 3 to Figure 7.

Surge and pitch RAOs have been compared with the experimental investigations performed by Wu (2013). Experimental data was available only in head waves. This comparison can be seen in Figure 3 and Figure 5. Surge motion is slightly over estimated as compared to experimental values.

DOI: 10.1016/j.oceaneng.2016.06.034

Using the motion response of the vessel, added resistance coefficients have been calculated using the method by Loukakis and Sclavounos (1978) (which is an extension of the classical Gerritsma and Beukelman's method) implemented in ShipX Veres. Calculated added resistance coefficients can be seen in Figure 8 along with the experimental values by (Wu 2013). Using these added resistance coefficients, added resistance was then computed in irregular waves for different peak frequencies and wave directions using the Pierson Moskowitz wave spectrum.

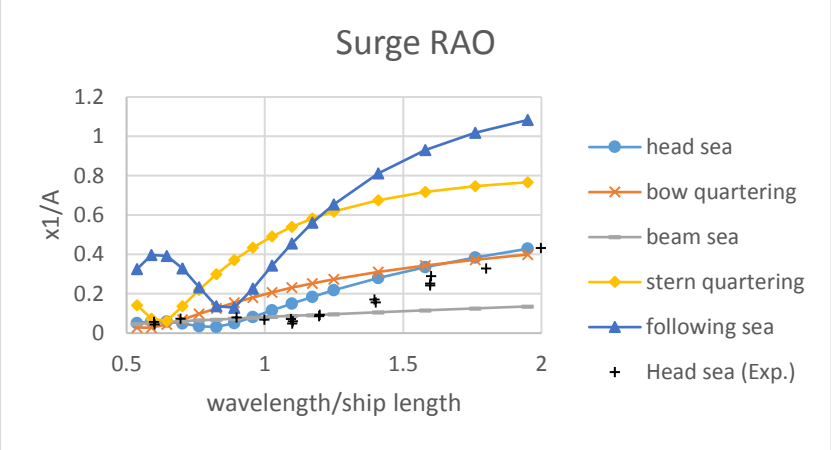

Figure 3 Surge RAO of KVLCC2 hull in different wave conditions with experimental validation

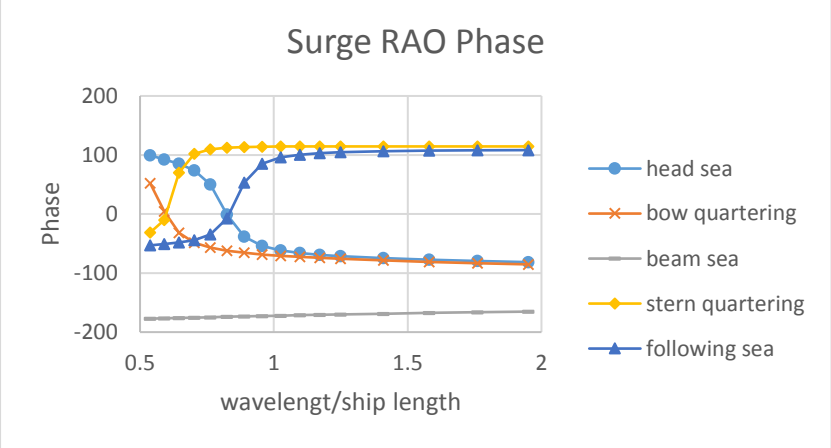

Figure 4 Phase of surge RAO of KVLCC2 hull in different wave conditions

DOI: 10.1016/j.oceaneng.2016.06.034

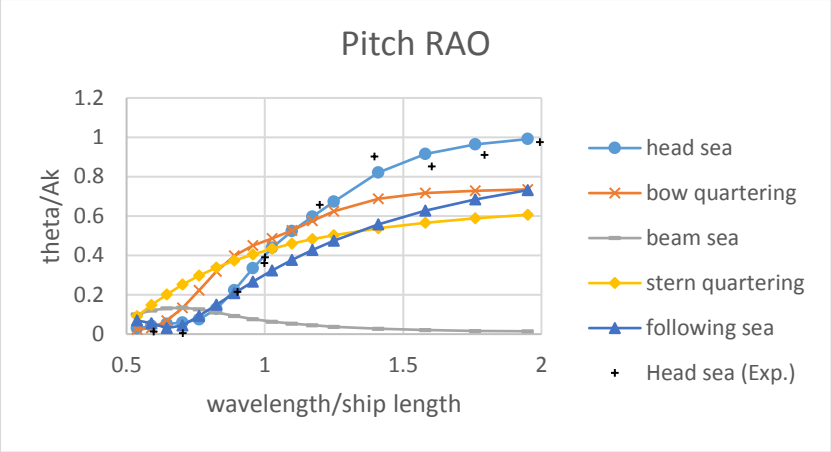

Figure 5 Pitch RAO of KVLCC2 hull in different wave conditions with experimental validation

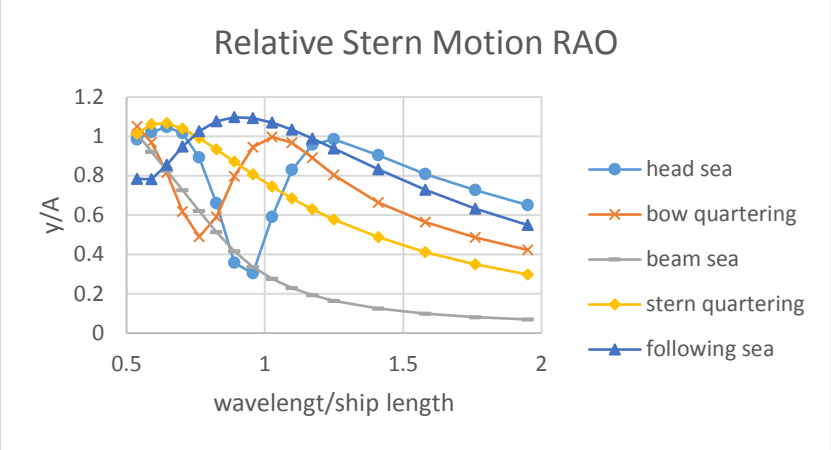

Figure 6 relative stern motion RAO of KVLCC2 hull in different wave conditions

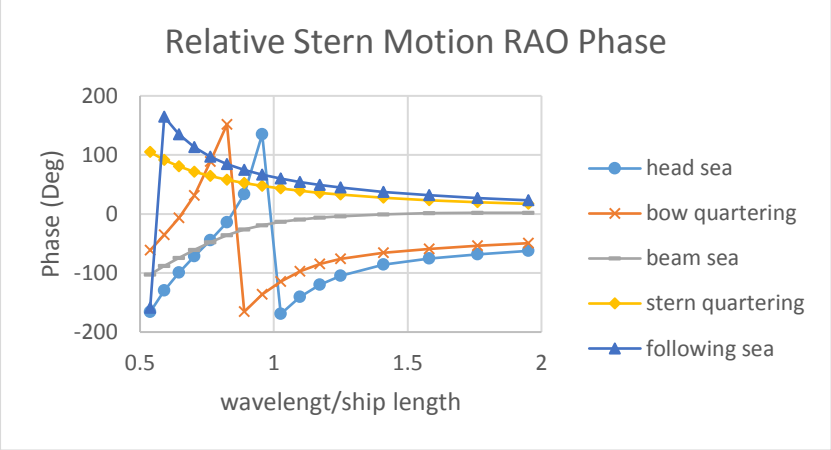

Figure 7 Phase of relative stern motion RAO in different wave conditions

DOI: 10.1016/j.oceaneng.2016.06.034

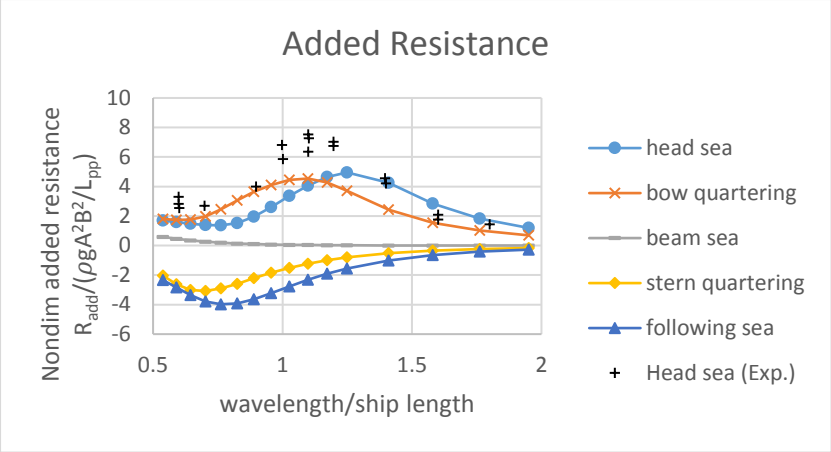

Figure 8 Added resistance in irregular waves of different peak wavelengths for KVLCC2 hull in different wave conditions.

5 Marine diesel engine details

The engine model selected for the simulation is Wartsila 8RT-flex68D. There is no engine specified for KVLCC2, and this one was selected partly based on availability of the model. The engine particulars can be seen in Table 3. The detailed information of the engine can be found from the project guide for the specific engine. Also the engine performance in terms of fuel consumption, power, mass flow, pressure and temperature are available from the manufacturer's website (WÄRTSILÄ 2014). These performance data are used in order to validate the engine system model.

Table 3 Engine particulars

Model	Wartsila 8RT-flex68D
Bore (mm)	680
Rated MCR (kW)	25,040
Speed at rated power (RPM)	95
Stroke (mm)	2720
Mean Effective Pressure (bar)	20
Number of cylinders	8
Turbocharger	2 x ABB A175-L35

DOI: 10.1016/j.oceaneng.2016.06.034

6 Simulation model

Engine and propeller models have been coupled using an inertial shaft model. Time dependent wake and shaft speed are inputs to the propeller model, which computes thrust and torque. Thrust is used by the vessel model to update the ship speed based on ship resistance and inertia. Torque is used by the shaft model to compute new shaft speed depending on shaft inertia and net torque applied to the shaft. Shaft speed is fed to the engine model to obtain torque produced at that speed and fuel injection commanded by the controller. An engine controller is used to control the fuel injection to the engine to keep engine speed constant and to avoid any over speeding. The overall model can be seen in Figure 9. Details of the modelling blocks are given further down.

The simulation model has been implemented in Matlab Simulink™ for overall integration of the submodels. A variable step solver (ODE45) has been used in order to capture transient dynamics of the overall system.

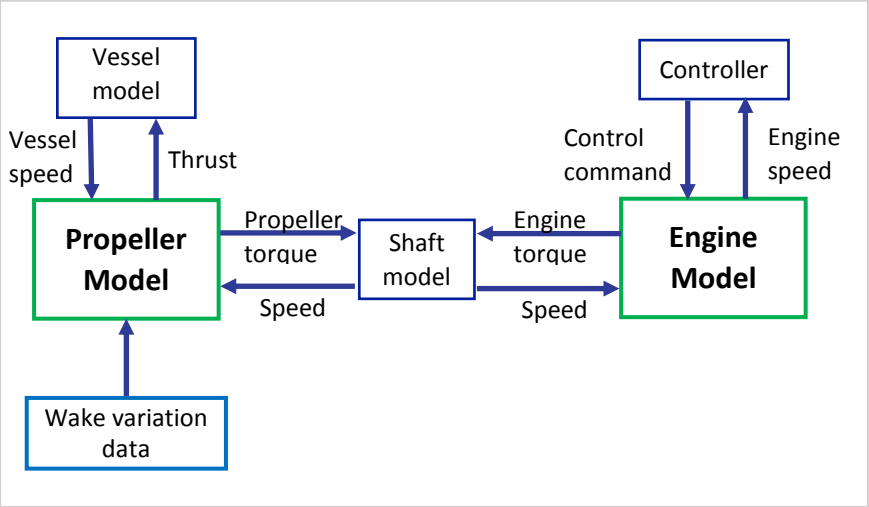

Figure 9 Overall model used for engine-propeller coupled simulations

6.1 Propeller model

For the propeller analysis, the open-source program Openprop based on vortex lattice lifting line theory (Epps 2010) has been used. It requires blade section details, frictional drag coefficient and wake

DOI: 10.1016/j.oceaneng.2016.06.034

velocities at each radial section. Frictional drag coefficients were obtained using *Javafoil (Hepperle)*, which uses a panel method to calculate velocity profile and pressure distribution over the foil section. Using these velocity and pressure distributions, boundary layer calculations are performed. Drag is calculated using momentum loss in the boundary layer.

In order to validate the Openprop results, open water curves obtained from Openprop were compared with the experimental open water data of original KVLCC2 propeller design. Good comparison between Openprop results and experimental results can be seen in Figure 10. Full-scale open water curves were obtained for the new propeller design for the calculation of thrust and torque at given propeller speed and ship speed, which means open water curves were used for the calculation of thrust and torque based on ship speed, propeller RPM and wake. Relative rotative efficiency has been assumed equal to one in all the cases.

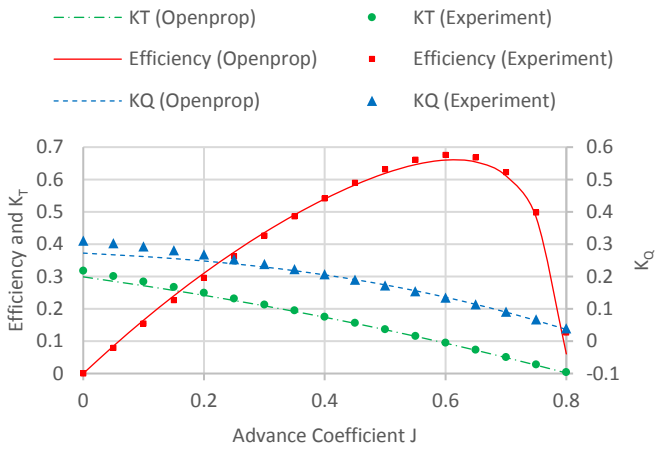

Figure 10 Comparison of Openprop and open water data of KVLCC2 propeller

In order to consider the effect of waves on the propulsion of the ship, thrust and torque losses due to propeller emergence, free surface effect and Wagner effect have been modeled. Thrust loss in case of propeller emergence has been assumed proportional to the out of water area of the propeller disc as suggested by Faltinsen, Minsaas et al. (1980). In case of propeller emergence, propeller blades take some time to develop the lift once they re-enter the water and thereby reducing average thrust and torque.

This effect has been considered in terms of average thrust and torque loss as suggested by Minsaas, Faltinsen et al. (1983). In addition, thrust and torque is lost when the propeller operates close to free surface generating waves on the free surface due to propeller action. These effects have been formulated using thrust diminution factor given by Minsaas, Faltinsen et al. (1983) as follows-

$$\beta = \begin{cases} 1 - 0.675\left[1 - 0.769\left(\frac{h}{R}\right)\right]^{1.258} & \frac{h}{R} < 1.3 \\ 1, & \frac{h}{R} \geq 1.3 \end{cases} \quad (1)$$

β is multiplied with the propeller thrust to obtain diminished thrust due to the effect of proximity to free surface.

The effects have been considered in quasi-steady sense as propeller depth varies much slower than its rate of rotation. Thrust and torque are considered varying in wave frequency, and higher harmonics have been ignored. These higher harmonics are mostly filtered away by the inertia of the shaft and propeller, and it is found that they do not affect the engine operation.

6.2 Procedure to estimate propeller inflow velocity

As mentioned earlier, one of the obstacles in the analysis of engine-propeller interaction in different weather conditions is the limited availability of wake data. Thus in order to simulate a variety of cases it is necessary to estimate wake in different wave-conditions.

Nakamura and Naito (1975) have shown that in presence of waves and ship motions, wake velocities fluctuate. Moreover, the mean of these fluctuations is different from the calm water wake. Hence, in presence of waves, mean wake changes along with the fluctuations. Ueno, Tsukada et al. (2013) have demonstrated that fluctuating wake velocities are caused by the wave induced particle motion and surge motion of the ship. Therefore, they state that wake velocities can be calculated as follows-

$$V_{fluctuating} = (1 - w_P)\{U - \omega_e \xi_a \sin(\omega_e t - \zeta_\xi)\} + \alpha\omega h_a \exp(-kz_P)\cos X \cos(\omega_e t - kx_P \cos X) \quad (2)$$

where,

$$\alpha = \begin{cases} 0.2\left(\frac{\lambda}{L|\cos X|}\right) + 0.5, for \ \frac{\lambda}{L|\cos X|} \leq 2.5 \\ 1, \qquad\qquad\qquad for \ \frac{\lambda}{L|\cos X|} > 2.5 \end{cases} \quad (3)$$

The coefficient α is different from 1.0 in case of head and bow-quartering waves since the waves reaching the propeller are modified due to the presence of the hull in front of it (Ueno, Tsukada et al. 2013). However, in case of following and stern quartering waves this coefficient is not required as the waves are directly felt by the propeller without significant disturbance from the hull. This means that we assume that the effect of reflected waves is negligible when it comes to wave induced fluctuations felt by the propeller.

Faltinsen, Minsaas et al. (1980) have proposed that the increase in mean propeller inflow (wake) due to the pitching motion of ship observed by Nakamura and Naito (1975) is caused by potential flow effects. Wake velocities due to the pitching motion of the ship can be calculated assuming the bottom of the ship to be a flat plate. Wake velocities can then be obtained as follows-

$$V_{mean} = \sqrt{\left(1 - \frac{\Delta\bar{p}}{0.5\rho U^2}\right)}\ U \quad (4)$$

where,

$$\Delta\bar{p} \sim -\frac{\rho}{4}\omega_e^2 |\eta_5|^2 x^2 \quad (5)$$

Comparison between mean increase in propeller inflow calculated by this method and that observed in the CFD can be observed in Table 4. Although there is a difference in the exact values between the calculation and experiment, trends are correctly predicted by the calculation.

Table 4 Comparison of increase in mean propeller inflow using formula and experiments

$\frac{\lambda}{L}$	A	% increase in mean wake velocities	
		(Calculation)	(Experiment)
0.6	3	0.03	0
1.1	3	2.70	5.0
1.6	3	2.66	2.2

Therefore, time varying total wake velocity in waves considering mean increase as well as fluctuations can be calculated as-

$$V_{total} = \Big((1-w_P)\{U - \omega_e \xi_a \sin(\omega_e t - \zeta_\xi)\} + \alpha\omega h_a \exp(-kz_P)\cos X \cos(\omega_e t - kx_P \cos X)\Big) * \sqrt{\left(1 - \frac{\Delta\bar{p}}{0.5\rho U^2}\right)} \quad (6)$$

Time varying wake velocities computed by equation (6) were then compared with the wake velocities obtained from the wake data in waves. Comparison can be seen in Figure 11. Due to good match between predicted and observed wake variation in waves, this formulation was used to obtain wake variations in different wave conditions. This made it possible to simulate engine propeller dynamics in presence of waves of various wavelengths, waveheights and wave directions, without being restricted to the conditions of the model test by Sadat-Hosseini, Wu et al. (2013).

Although these simple methods might not be accurate in all the conditions, they can certainly be used to access the possible effect of waves on the propulsion in waves before going for more accurate but time consuming analysis.

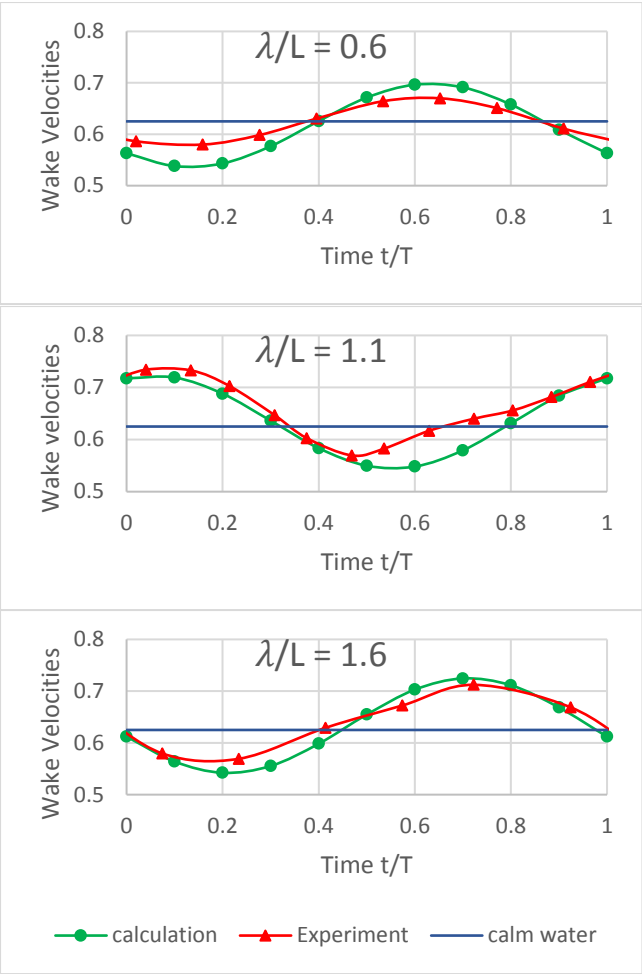

Figure 11 wake variation procedure vs experimental wake

6.3 Vessel model

The following vessel model has been implemented to include vessel dynamics in the simulations-

$$(m + m')\ddot{x} = (1 - t')T' - (0.5\rho S C_T \dot{x}^2 + R_1) \quad (7)$$

Although thrust deduction varies in presence of waves (Moor and Murdey 1970), it has been considered to be constant and equal to its calm water value, due to the lack of knowledge about how thrust deduction vary in presence of waves for this particular ship. R_1 and $T'$are the only time dependent inputs that are updated each time step. The added resistance coefficient was modeled as a function of ship speed as it varies with ship speed. The added resistance coefficient was computed for different ship

DOI: 10.1016/j.oceaneng.2016.06.034

speeds from 9.5 knots to 15.5 knots in each wave condition and it was curve-fitted with second order polynomial of ship speed. One such curve fitting in case of irregular head waves with peak frequency equal to that of wave λ/L=1.1 can be seen in Figure 12.

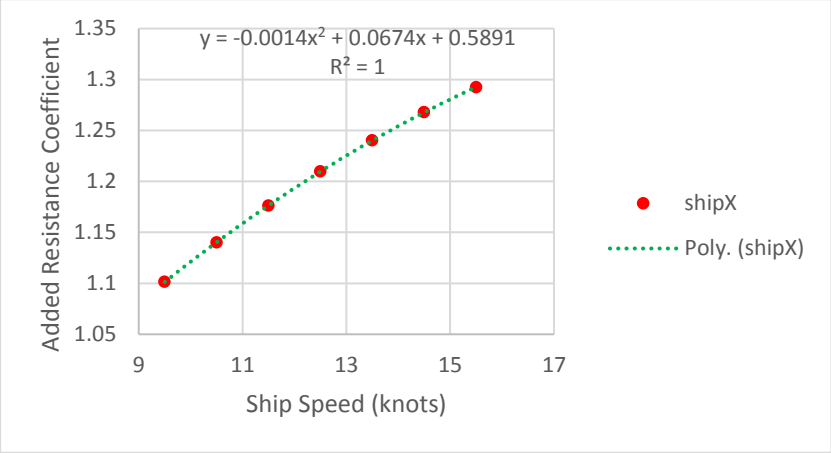

Figure 12 Dependence of added resistance coefficient on vessel speed

Simulations have been performed to analyze the interaction of regular waves with the propulsion unit. However, added resistance has been calculated in irregular waves of significant waveheight equal to the waveheight of the regular wave and peak frequency same as the frequency of the regular wave. This is done to keep the analysis simple and yet keep ship resistance and engine load realistic. Therefore, simulation conditions are similar to the ship travelling in irregular waves and encountering a wave train of regular waves.

6.4 Propulsion shaft model

The shaft is assumed to be rigid and the quadratic friction model is used. Mass moment of inertia is assumed to be twice as much as that of the engine ($J_{Shaft} = 323000kg.m^2$). The dynamic equation for the shaft is given as:

$$J_{Shaft}\dot{\omega}_{Shaft} = \eta_m(\omega_{Shaft}).Q_{Eng} - Q_{Load} \quad (8)$$

where η_m is a mechanical efficiency of the engine crank system and the propulsion shaft, given as an empirical function:

DOI: 10.1016/j.oceaneng.2016.06.034

$$\eta_m = 1 - a_2\omega_{Shaft} + \frac{a_1}{1-a_2}(a_2\omega_{Shaft} - {\omega_{Shaft}}^2) \quad (9)$$

6.5 Marine diesel engine model

The purpose of the engine system model in this paper is: (1) to provide dynamic shaft torque and (2) to predict the cycle efficiency of the engine under transient conditions. The transient load from the propeller changes both torque and speed, causing highly nonlinear behavior of the system. Therefore, the engine system model should include the physical process of the essential components of the engine system, namely turbocharger, air coolers, air/exhaust receiver volumes and engine cylinder blocks in order to predict nonlinear and transient aspects of engine operation. The physical interface of the system is through the mechanical shaft where rotational speed is input to the engine model and torque is output. In addition, the engine model takes inputs from the engine controller, which are fuel rack position, valve timing, and injection timing.

The engine system model is based on the filling and emptying method, which is most commonly used for engine system modeling (Rakopoulos and Giakoumis 2006). Filling and emptying method is a lumped parameter modeling approach where the system is divided into a finite number of uniform thermodynamic control volumes. Such a model is capable of simulating pressure and temperature in the component and flow between the components. Since we will observe system performance in terms of torque response as well as efficiency, more detailed methods like gas dynamic model (Takizawa, Uno et al. 1982) or multi-zone model (Hiroyasu, Kadota et al. 1983) are not required. In addition, the engine contains large receiver volumes before and after the cylinder, which smooths pressure fluctuations entering the engine cylinder and turbine. This further justifies the use of a filling and emptying model.

In a filling and emptying method, all components are grouped into two categories: control volume and flow restriction. In a control volume, mass and energy are accumulated depending on the net flows and the thermodynamic properties are determined in the volume. It is assumed that such properties are

uniform in the volume. On the other hand, flow restriction allows mass and energy to flow between two control volumes or between a control volume and environment. It is assumed that there is no mass and energy accumulated in restrictions. Any physical flow restriction like valves, ports, and orifices are grouped in this category. In addition, a cooler or turbomachinery can be grouped in this as a simplified model.

Three common groups of system variables are used inside the thermodynamic part of the engine model and their interfaces, namely thermodynamic states, mass and energy flows. As the main part of an engine system is a thermodynamic process of gas mixture, thermodynamic states used in this work are pressure, temperature and the composition of the gas, for which we use fuel-air equivalent ratio, whereas mass flow of gas, enthalpy flow or rate of change in internal energy and mass flow of burned-fuel are flow variables. In case of varying volume, the rate of change of volume should also be included in the flow variables.

The input to a flow restriction element is a set of thermodynamic states (p, T, F) of adjacent control volumes and the output is a set of mass and energy flows $(\dot{M}, \dot{E}, \dot{M}_{\mathrm{b}})$ determined depending on the specific process of the component. For example, isentropic compressible flow equation through a restriction (Heywood 1988) is used for valve, orifice or port whereas a performance map is used for a compressor and a turbine. On the other hand, a control volume has the input of a set of flows from connected flow restrictions and output of the thermodynamic states. The first law of thermodynamics and mass conservation is used to calculate the net rate of change in mass and energy in the control volume. Those net rate of changes are integrated to find the mass and energy of the volume $(M, E, V, M_{\mathrm{b}})$. Then, we used Zacharias' correlation (Zacharias 1967) for thermodynamic properties of the combustion gas and the ideal gas law to algebraically obtain the thermodynamic states (p, T, F). In addition, if the control volume is connected to a mechanical component, it will have an additional input of rate of volume change and a pressure output on this interface.

DOI: 10.1016/j.oceaneng.2016.06.034

The system model is assembled from the model libraries of components developed by the authors. Then, the block diagram of the overall system looks like in Figure 13.

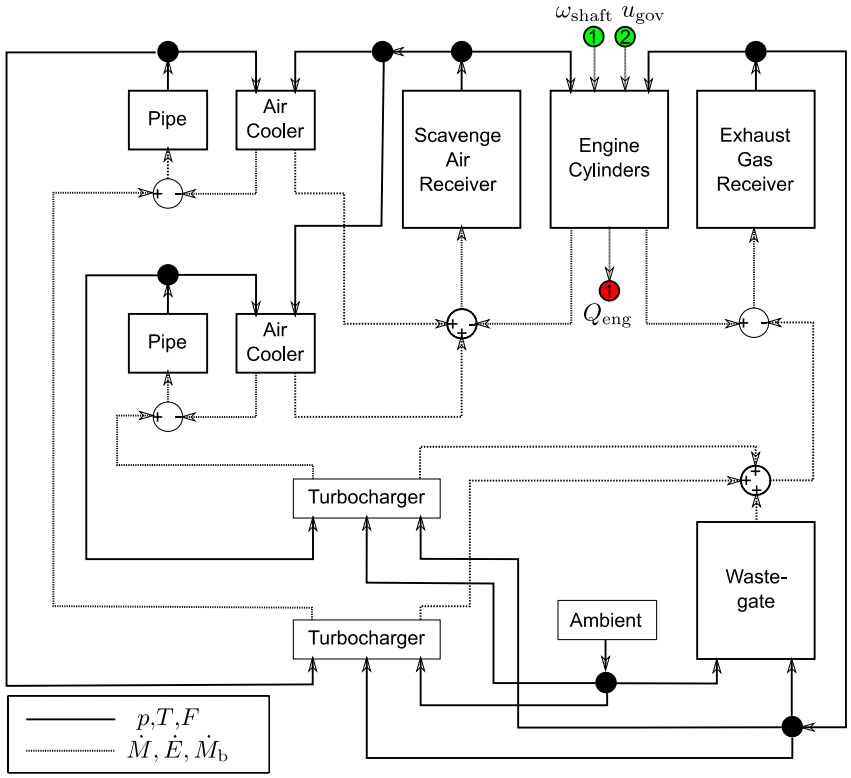

Figure 13 Block Diagram of the Engine System Model

The simulation model has sub-models to describe the specific physical process in the internal combustion engine. For the combustion in the cylinder, a Wiebe function is used with fixed parameters to describe the rate of heat release. An ignition delay model is also included, which correlates the delay to pressure and temperature of the cylinder. For the gas exchange process, a scavenging model suggested by Sher (1990) is adapted to a single-zone model. For the turbochargers, a quasi-steady approach was used where flow and efficiency are obtained from the performance map provided by the manufacturer. For the heat transfer, the model by Woschni (1967) was used to predict the heat transfer coefficient whereas radiation was neglected. Heat transfer from the radiation was not separately computed but included in the overall heat transfer model. For the heat exchanger model, effectivity-the NTU model was used (Incropera, DeWitt et al. 2007).

DOI: 10.1016/j.oceaneng.2016.06.034

The engine system model was then validated against the steady state performance data provided by the engine manufacturer. The engine system model for validation is connected with a shaft model described in the paper. A simple propeller model is also used as a quadratic curve between torque and speed. The propeller curve was derived from the power and engine speed relation given in the engine performance data. From numerous simulations, we found that brake specific fuel consumption (BSFC) is well-correlated with maximum cylinder pressure. Since the combustion profile described by the Wiebe function is fixed, we could regulate the maximum cylinder pressure by changing exhaust valve close (EVC) timing and injection timing. Early exhaust valve closing will make apparent compression ratio high and vice versa. Also retarded fuel injection may enable keeping high compression ratio without exceeding permissible maximum cylinder pressure. In this work, a controller was devised to set a reference maximum cylinder pressure from comparison of measured BSFC and the reference value. While the firing pressure, which is the pressure differential between maximum cylinder pressure and compression, was kept constant by regulating fuel injection timing, the compression pressure was controlled to the reference value by regulating exhaust valve timing.

From the simulations at difference loads, the EVC timing and fuel injection timing were obtained to achieve the reference BSFC. In addition, other performance data were compared to the reference data and they generally show good fit as shown in the Figure 14.

DOI: 10.1016/j.oceaneng.2016.06.034

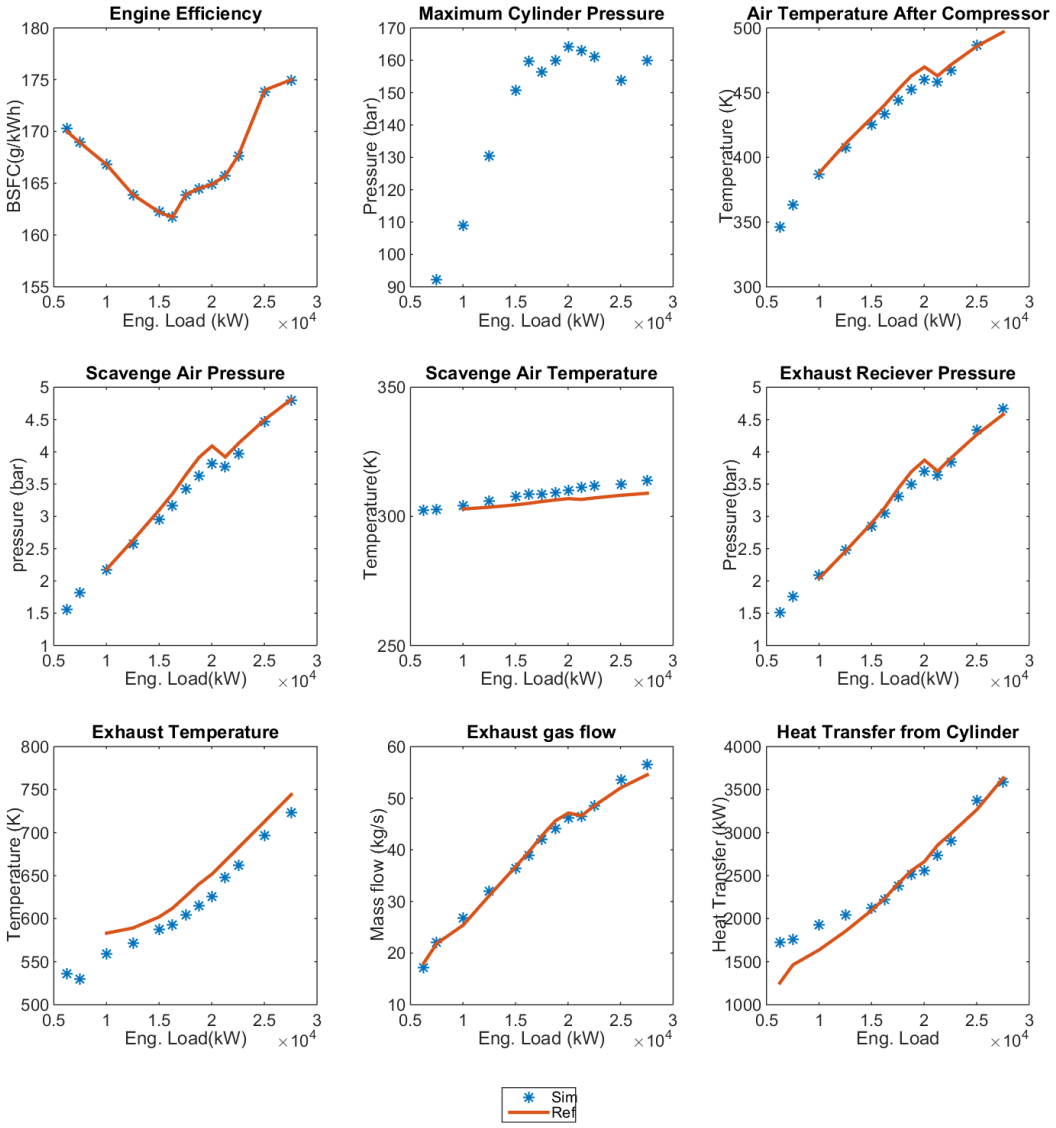

Figure 14 Diesel Engine Steady State Simulation

For the transient simulation model, the EVC timing and fuel injection timings are parametrized into a table with reference engine speed and the actual values are interpolated at given engine speed. For the governor, a PI controller is used to regulate the shaft speed to a reference value. The measured shaft speed is low-pass filtered in order to filter any noise and cylinder-to-cylinder variation. The controller is also tuned so that the system has reasonably fast response while avoiding oscillation. While tuning the control parameters, a sensitivity analysis was performed in order to see the influence of the variation in the uncertain parameters. As a result, it was found that the mass moment of inertia of the shaft, among

other parameters such as proportional gain of the controller and turbocharger inertia, has a negligible influence on the time constant of the engine speed response to the step change in speed command. This result justifies using rough estimation of inertia of the propulsion system.

However, the turbocharger shaft inertia has significant influence in case of a large step change in speed command because of the smoke limiter. This additional controller limits the fuel rack position depending on the charge air available in the cylinder. The amount of charge air available is predicted from the scavenge air receiver pressure and the volumetric efficiency of gas exchange process. As the rate of pressure development for load increase is delayed due to inertia of the turbocharger and filling the receiver volume, the fuel rack position from the governor saturates by this limit. This phenomenon is commonly referred as “turbo-lag”. Combination of both PI type governor and smoke limiter ensures reasonable response of the engine especially in case of abrupt change in load.

7 Engine-Propeller Coupled Simulations and results

Two sets of simulations were performed. Firstly, added resistance was excluded from the simulations in order to observe the effect of unsteady flow alone on the propulsion performance. Excluding the added resistance makes different cases directly comparable. Effect of waves on engine efficiency and propeller efficiency was separately studied along with their combined impact on vessel performance. Secondly, simulations were performed including the added resistance to simulate the situations that are more practical. Importance of wake change, engine-propeller interaction and thrust and torque losses in waves on power and velocity prediction of vessel was analyzed.

7.1 Simulations without added resistance

7.1.1 Engine-Propeller Dynamics in Waves

Power, speed and torque variations in presence of head sea can be seen in Figure 15, Figure 16 and Figure 17. Power variations in wave λ/L = 1.1 are larger as compared to those in λ/L=0.6. This can be explained by the fact that larger waves reach the propeller without much decrease in amplitude as compared to smaller waves. In case of λ/L=1.6, distinct sharp peaks in shaft speed are caused by propeller emergence, causing sharp drops in torque seen in Figure 17.

High frequency fluctuations in torque and shaft speed (appearing as thick lines in the graphs) in Figure 16 and Figure 17 are due to the firings of individual cylinders. These can be clearly seen in the instantaneous engine power plot in Figure 18.

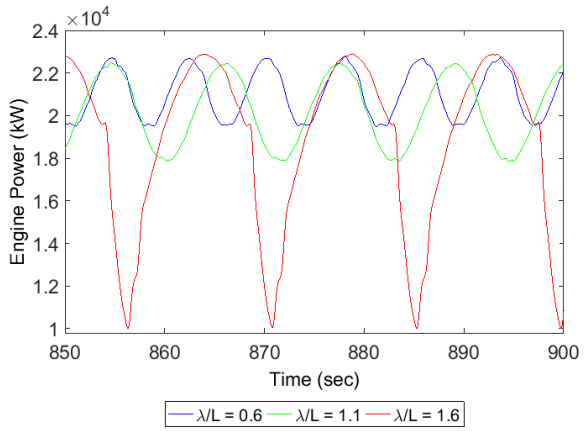

Figure 15 Low frequency engine power fluctuations in presence of three different head waves of 5 m wave amplitude

DOI: 10.1016/j.oceaneng.2016.06.034

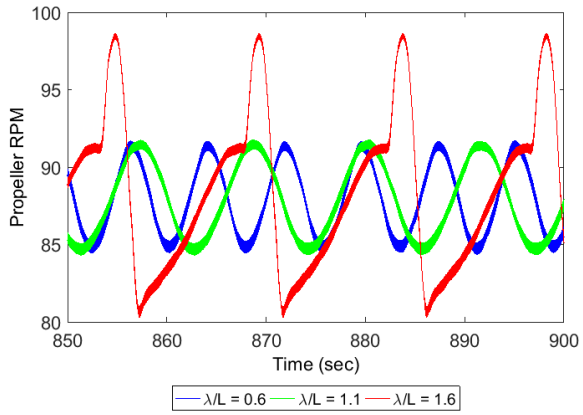

Figure 16 Engine speed fluctuations in presence of three different head waves of 5 m wave amplitude

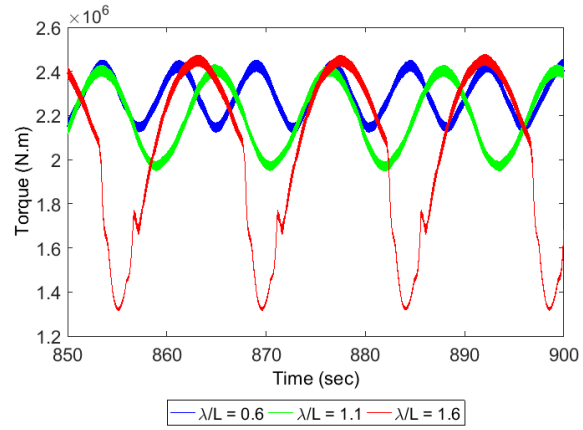

Figure 17 Propeller torque fluctuations in presence of three different head waves of 5 m wave amplitude

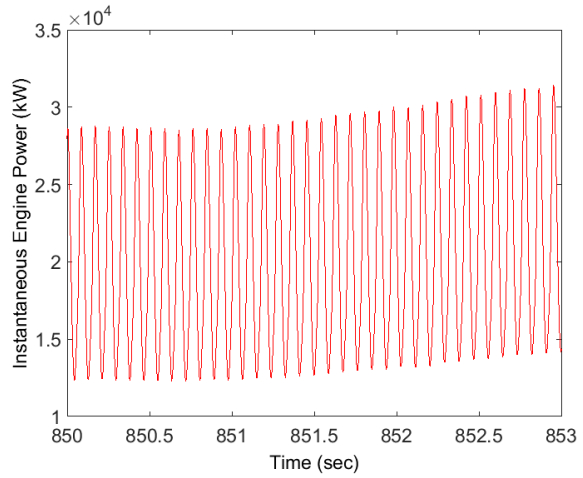

Figure 18 High frequency power variation due to individual cylinder firing

DOI: 10.1016/j.oceaneng.2016.06.034

7.1.2 Engine propeller coupled model vs constant propeller speed assumption

Propeller speed is often assumed constant in the investigation of variation in the propeller forces and propeller performance to avoid the complexity of engine-propeller coupling. To check the validity of this assumption, simulations were run without the engine model assuming constant propeller speed. Torque and power variations obtained using fixed speed in head wave were then compared with those obtained using the coupled model. For the fixed speed calculations, engine power is computed simply as torque times propeller speed.

Comparison of power and torque variations with and without engine model can be seen in Figure 19 and Figure 20 in the event of propeller emergence. Variation in torque and power is higher in case of constant speed assumption whereas, when engine model is included, torque and power variation reduces due to the combined effect of the diesel engine response and control system. The phase difference seen in the figures is incidental, not due to real differences in the two models.

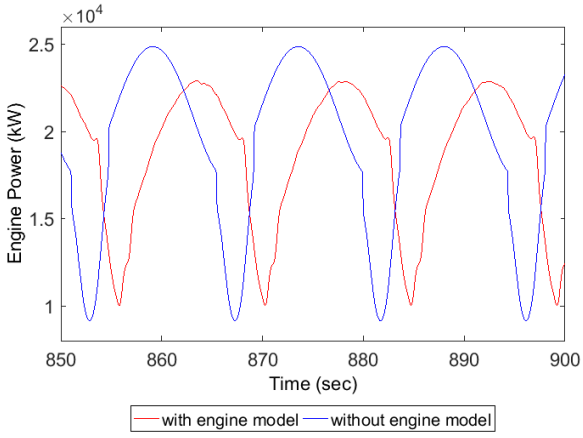

Figure 19 Low frequency engine power variation with engine model and with constant speed assumption in wavelength λ/L=1.6 and 5 m wave amplitude

DOI: 10.1016/j.oceaneng.2016.06.034

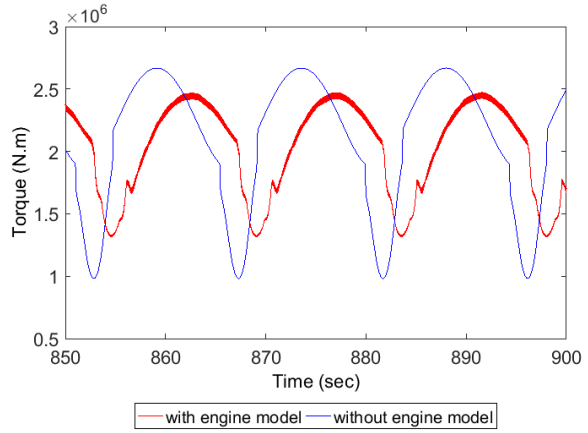

Figure 20 Torque variation with engine model and with constant speed assumption in wavelength λ/L=1.6 and 5m wave amplitude

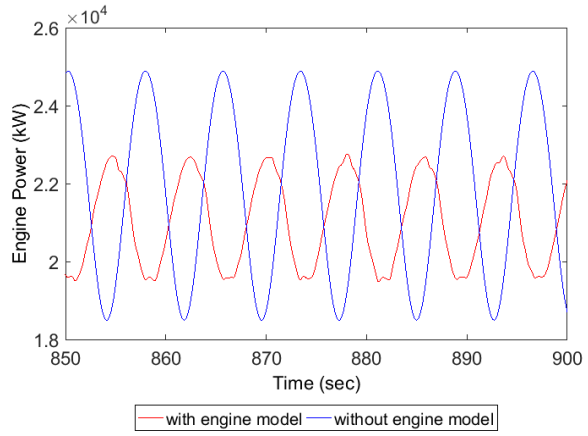

Figure 21 Low frequency engine power variation with engine model and with constant speed assumption in wavelength λ/L=0.6 and 5 m wave amplitude

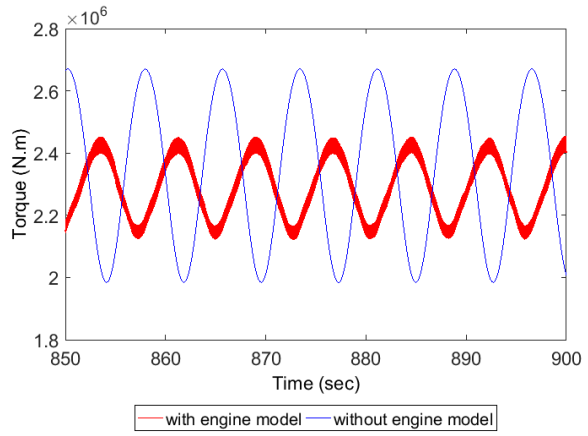

Figure 22 Torque variation with engine model and with constant speed assumption in wavelength λ/L=0.6 and 5 m wave amplitude

DOI: 10.1016/j.oceaneng.2016.06.034

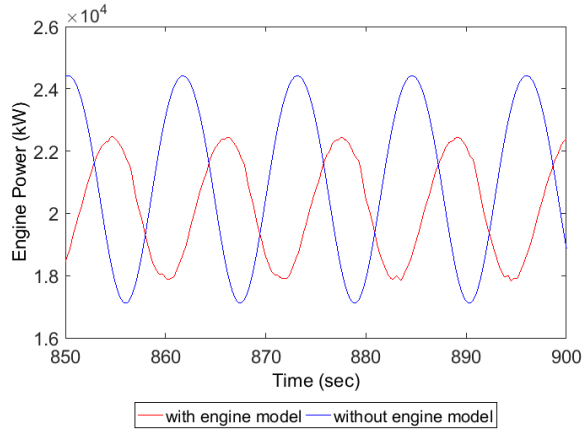

Figure 23 Low frequency engine power variation with engine model and with constant speed assumption in wavelength λ/L=1.1 and 5 m wave amplitude

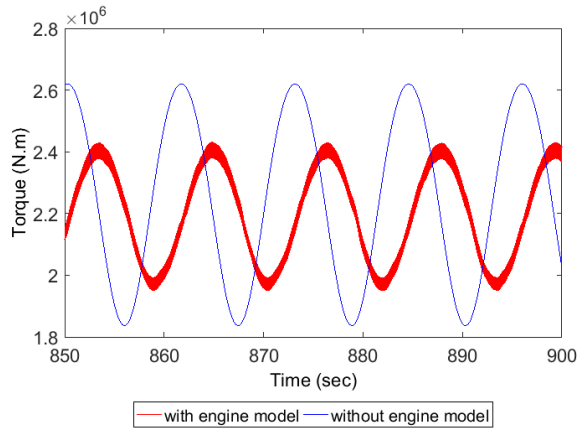

Figure 24 Torque variation with engine model and with constant speed assumption in wavelength λ/L=1.1 and 5m wave amplitude

Similar comparisons can be seen in other wavelengths (λ/L=0.6 and λ/L=1.1) in Figure 21 to Figure 24 without propeller emergence. In all the cases, power and torque fluctuations are lower in case of the simulations with a diesel engine model. However, the ratio of power and torque fluctuations with and without a diesel engine model is different in each case due to different response of the system to different load frequencies.

It is, however, important to note that torque and power variations are qualitatively similar with and without a diesel engine model. Hence, if relevant effects like wake variation, ship motion and propeller depth variation are included, then the simulations without a diesel engine model will give conservative

estimates of variation in propeller forces, torque and power. However, for accurate estimates of system response the coupled engine propeller model should be used.

7.1.3 Engine-propeller dynamics in the event of propeller emergence

As we know, over-speeding is detrimental for the diesel engine. Thus, for safety purpose, the fuel supply to the diesel engine might be shut off in an event of over-speeding, eventually tripping the unit. The control system is designed such that even in rough weather the engine operates within the range of safe operating speed. However, events like propeller emergence can cause sharp increase in speed. The amount of speed overshoot before the control system kicks in to limit the fuel injection is important to investigate. For this investigation, coupled engine-propeller simulations are required as propeller torque variation at different propeller immersions, ship motions and engine reaction play important roles in such an event. This will also tell us if the propeller-engine system with the given control-strategy is safe in the event of propeller emergence. If the system is found to limit the over-speeding, it would allow us to keep the engine running at high power even in relatively harsh weather without the danger of causing damage to the engine.

The event of propeller emergence observed in wave λ/L=1.6 with 5m wave amplitude has been studied in detail. Simulation in the same wavelength with 6m wave amplitude has been carried out to study larger propeller emergence where, as much as half of the propeller disc comes out of water (i.e. propeller submergence ≈ 0). Variation of torque, engine power, propeller speed and propeller submergence has been plotted in both the cases as seen in Figure 25.

DOI: 10.1016/j.oceaneng.2016.06.034

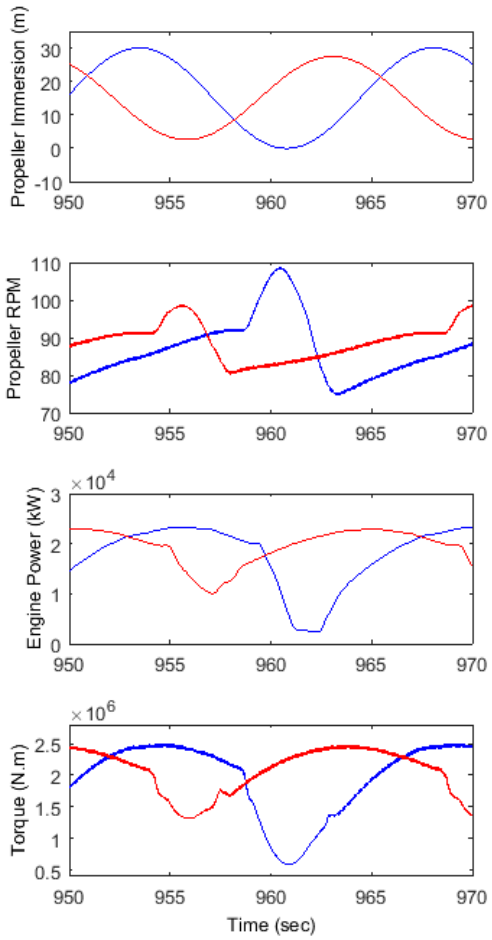

Figure 25 Propeller emergence in wavelength λ/L=1.6 in wave amplitudes 5m (red) and 6m (blue)

Torque drops sharply as soon as propeller starts coming out of water and propeller speed starts to increase. Minima in torque and maxima in speed occurs when the propeller submergence is minimum (i.e. maximum part of propeller is out of water) as expected. At this point, power continues to fall, reaching its minimum when the propeller is fully submerged again. These trends can be observed in both the cases of propeller emergence.

Assuming that up to 10% over speeding of the engine is safe; the control system successfully limits the engine speed in 5m wave amplitude. Whereas in 6m wave amplitude, it fails to limit the propeller speed.

DOI: 10.1016/j.oceaneng.2016.06.034

Hence, in 6m waves, engine power has to be brought down in order to avoid engine shutoff in rough weather but in 5m waves, it is safe to keep the engine running at design speed.

We can conclude that such coupled simulations are capable of assessing the safety of the propulsion system and the performance of control system in different weather conditions beforehand. Therefore, such a framework can be effectively used to develop an efficient as well as safe engine control system.

7.1.4 Effect of waves on the overall propulsion system due to engine propeller dynamics

Currently, for speed loss and sea margin calculations only added resistance and change of propulsion point due to change in ship speed is taken into account as per ITTC (2008). Wake is assumed constant and propulsion system is assumed to perform like a steady state even in a dynamic flow field. Therefore, influence of time varying flow field on the performance of engine propeller system has been investigated.

The efficiency of the propulsion system can be divided into two parts, the efficiency at which fuel is converted into power i.e. efficiency of engine and the efficiency at which the engine power is used to propel the ship i.e. propulsive efficiency. Effect of waves on both the efficiencies has been investigated in waves encountered from different directions with three different wavelengths each with three different wave amplitudes. Here it is necessary to remember that added resistance was not included in these sets of simulations. These results have been presented considering the simulation in calm water condition to be the benchmark case. Wave direction has been considered to be the angle between the direction of propagation of wave and the heading of the ship. (0 degree is following sea; 180 degrees is head sea)

7.1.4.1 Change in Engine Efficiency

Variation in BSFC in different conditions as a result of load fluctuations due to waves can be observed in Figure 26. In all the cases, change in BSFC is relatively small. As mentioned in the control part of the diesel engine, the cycle efficiency of the engine highly depends on the timing of the exhaust valve or, in

other word, apparent compression ratio. Since the speed is controlled at a single reference value and the speed variations are relatively low, we could not observe meaningful deviation of the average cycle efficiency.

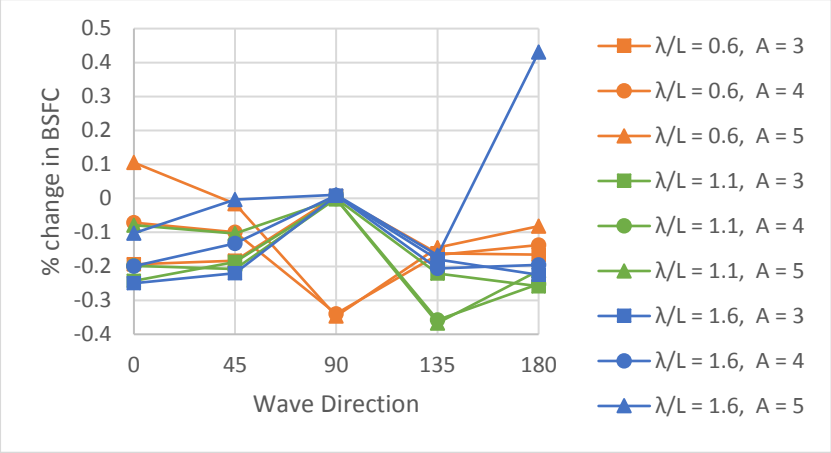

Figure 26 Increase in engine BSFC due to time varying propeller torque in different waves

7.1.4.2 Change in Propulsive Efficiency

All the simulated conditions show different power as well as ship speed at constant propeller speed setting, making it difficult to directly compare required engine power in different cases. Since there is no added resistance in this set of simulations, it would be meaningful to compare the ratio of power and the cube of the ship speed (the ratio that can be assumed constant in calm water). This ratio can give us an indication of propulsive efficiency. Increase in the ratio means that higher power is required compared to calm water operation to propel the ship at same speed. Percentage increase in the ratio of power and the cube of ship speed in presence of waves can be seen in Figure 27. Change is significant in case of head and bow quartering sea for λ/L=1.1 and 1.6. Whereas, λ/L=0.6 shows comparatively small change in any wave direction. This power loss is due to the combined effect of drop in propeller efficiency and change in hull efficiency as wake fraction changes in waves.

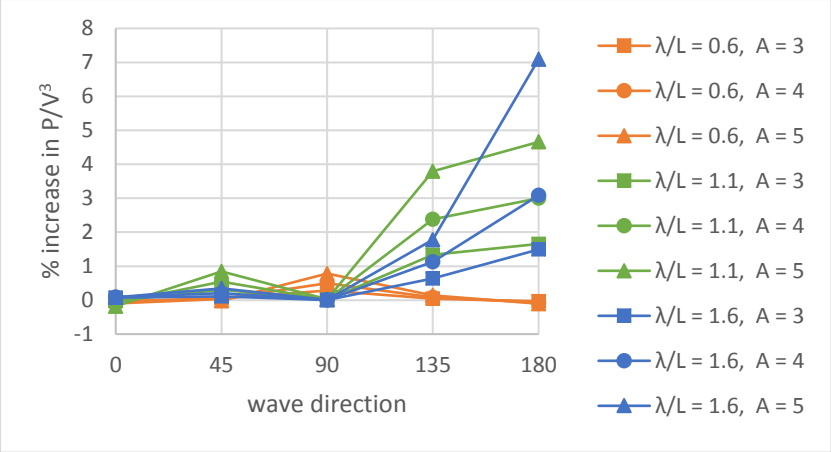

Figure 27 Change in the performance of propulsion system (engine + propeller) due to unsteady wake and propeller engine interaction

Change in propeller and hull efficiency has been studied separately to study how much each of these factors contributes to increase in P/V^3. Variation in propeller efficiency in different wave conditions can be seen in Figure 28.

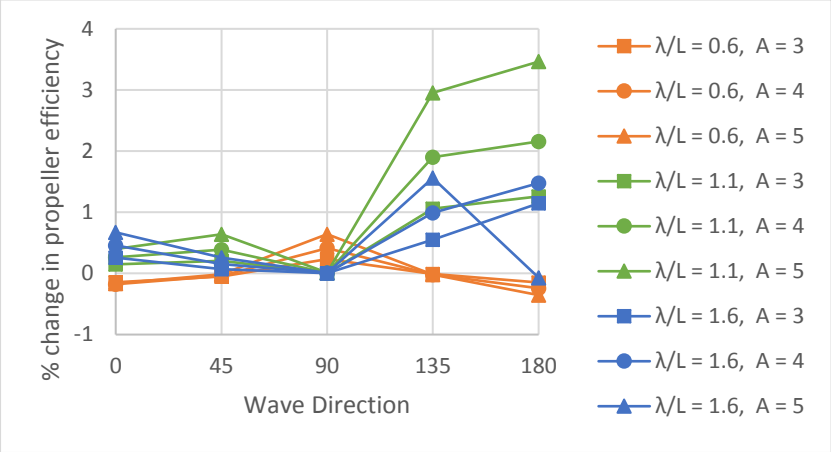

Figure 28 Change in propeller efficiency in different wave conditions due to time varying flow field

Change in the propeller efficiency can be attributed to two factors. One, due to variation in propeller speed because of time varying propeller inflow and engine dynamics; second, due to change in operating point of propeller because of mean change in wake velocities as a result of pitching motion of the ship. Increase in wake velocities increase the advance coefficient, leading to higher efficiency but lower thrust as compared to calm water condition. This can lead to drop in ship speed, which would reduce the

advance coefficient, since propeller speed is kept constant. Effectively it was observed that final advance coefficient in waves was higher than the calm water condition in most of the cases.

Propeller efficiency increases in head waves and bow quartering waves for λ/L=1.1 and 1.6. In these cases, the effect of increase in advance coefficient seems to dominate. Whereas, in head wave λ/L=0.6, small drop in advance coefficient together with dynamic shaft speed variation causes drop in efficiency. A similar trend is seen in following and stern quartering sea but the amount of increase in efficiency is much lower. These cases have relatively higher wake variation since wave induced particle velocities directly affect the propeller unlike in case of head waves, where the hull in front of the propeller reduces this effect.

Another part of the propulsive efficiency is the hull efficiency. The change in hull efficiency has been plotted in Figure 29. It can be observed that the drop in hull efficiency is more significant than the drop in propeller efficiency. It is a dominating factor causing change in the ratio of P/V^3. Moreover, since we have neglected change in thrust deduction due to waves, it can be concluded that accurate estimation of wake variation is essential for the performance estimation of the ship. However, engine dynamics has minor influence on change in propulsive efficiency in case of simulations without added resistance.

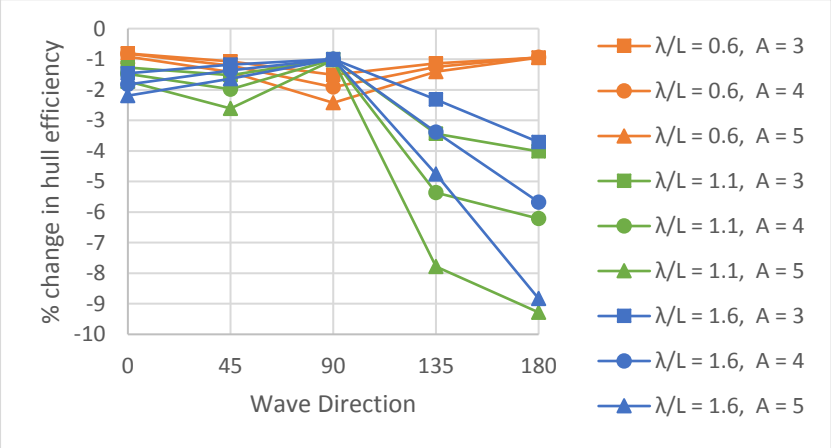

Figure 29 Change in hull efficiency due to time varying wake in waves

DOI: 10.1016/j.oceaneng.2016.06.034

7.2 Simulations with added resistance

Realistic cases were simulated by including the added resistance in the simulations to determine propulsion performance in waves. However, in these simulations, the performance of the ship is affected by added resistance as well as change in engine and propulsive efficiency, and it is difficult to separate the effects of the two.

7.2.1 Effect of waves on the engine performance

From comparison of Figure 30 with Figure 26, it can be seen that changes in BSFC are only slightly higher than those in case of simulations without added resistance. Therefore, even after including the added resistance, variation in BSFC is small in most of the wave conditions.

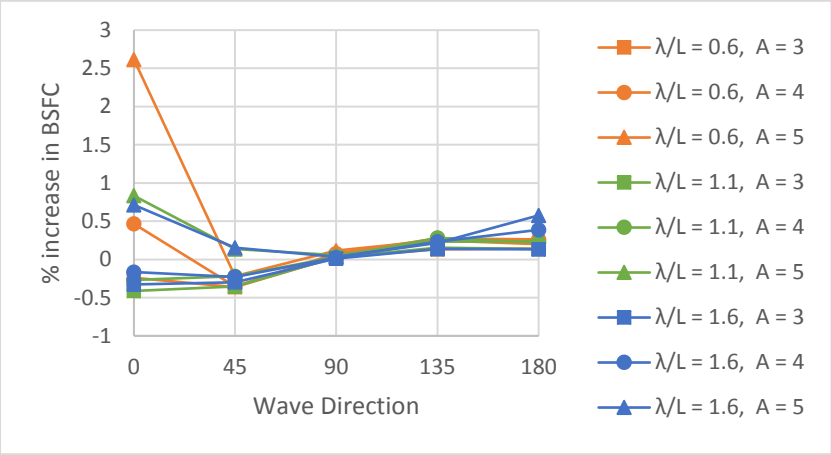

Figure 30 Increase in BSFC of engine due to combined effect of fluctuating load and change in power load due to added resistance in different wave conditions

7.2.2 Importance of engine-propeller coupled model in performance prediction in waves

Since it is difficult to separate the effects of added resistance from those of unsteady engine propeller dynamics and wake variation, another set of simulations were run without engine model. However, effects of wake variation, ship motion, thrust and torque losses were considered. The propeller speed was kept constant. Therefore, the difference between the simulation results with and without engine model is purely due to engine propeller dynamics. The simulation results have been compared in terms of quasi-propulsive efficiency and the ship speed achieved.

Difference between the quasi-propulsive efficiency with and without engine model can be observed in Figure 31. Changes in quasi-propulsive efficiencies are minor except in case of head and bow quartering waves of 5m wave amplitude where efficiencies are lower in case of simulations with engine model. In these cases, engine is operating close to 100% MCR where control system tries to constrain the engine power by limiting the fuel injection. This effect being absent in the simulations without engine model, leads to the differences in the performance prediction. This difference in the efficiencies causes difference between the ship speeds predicted by two simulations as seen in Figure 32.

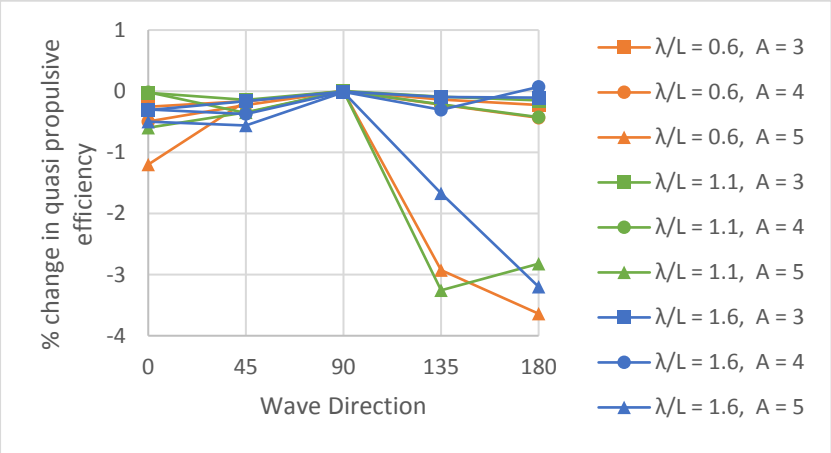

Figure 31 Percentage change in quasi-propulsive efficiency due to the use of engine model as compared to that without engine model (including wake change, thrust and torque loss calculations)

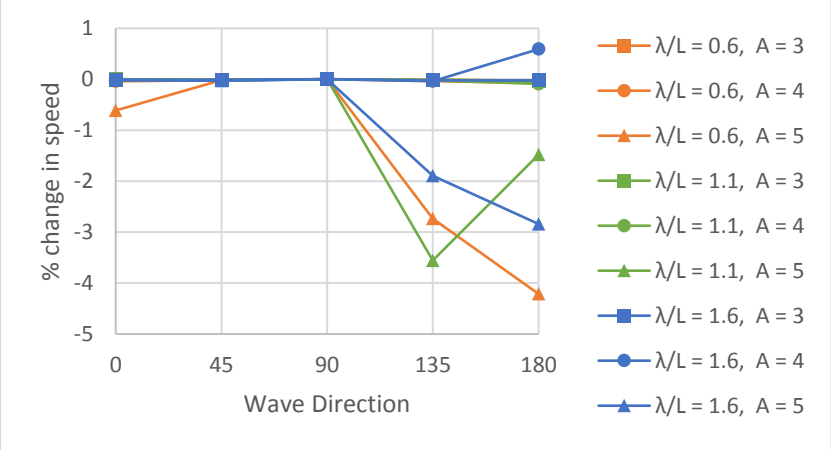

Figure 32 Change in the prediction of final ship speed including engine model as compared to that without engine model but including wake change, thrust and torque loss calculations

DOI: 10.1016/j.oceaneng.2016.06.034

Simulations were also run without engine model, without considering wake variations and change in thrust and torque in order to analyze the importance of considering wake change and propulsion losses. These simulations without engine model resemble the traditional calculations performed to analyze ship in waves, where effect of waves is taken into account only in terms of added resistance and change of propulsion point. In most of the cases, vessel speed predictions in these cases are even higher than the simulations without engine model including wake variation and thrust, torque losses. Therefore, as compared to these cases, simulations with engine model predict much lower ship speeds as seen in Figure 34. Significant difference can also be observed in quasi-propulsive efficiency in Figure 33.

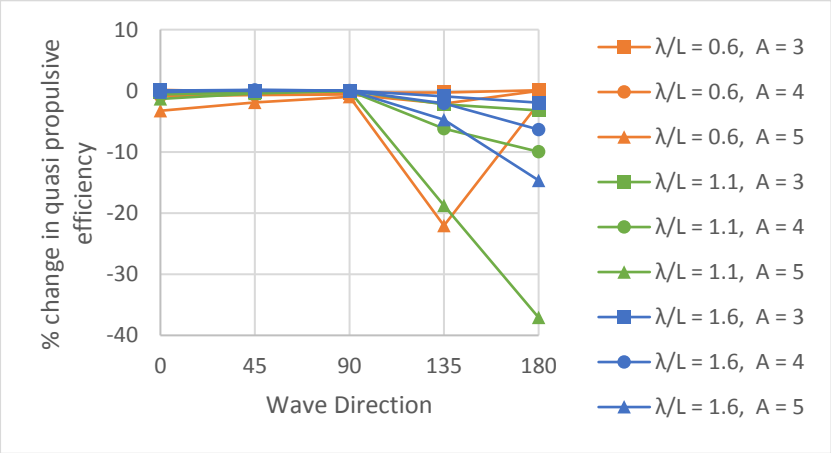

Figure 33 Percentage change in quasi-propulsive efficiency due to the use of engine model as compared to that without engine model without considering wake change and changes in thrust and torque

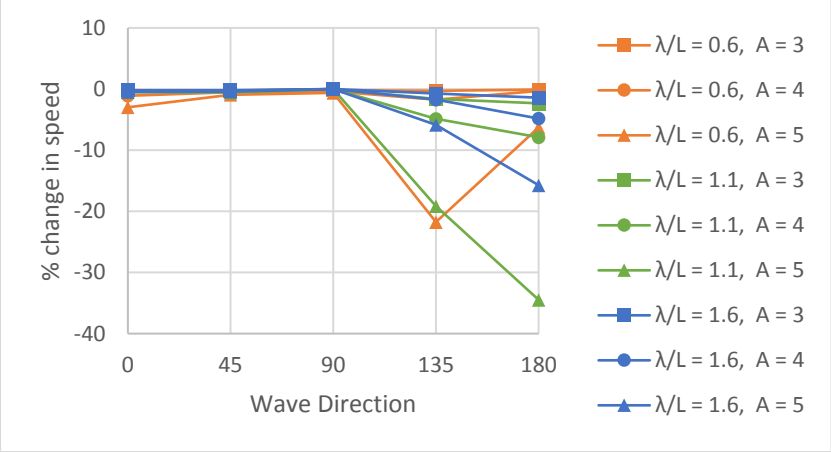

Figure 34 Change in the prediction of final ship speed including engine model as compared to that without engine model without considering wake change and changes in thrust and torque

DOI: 10.1016/j.oceaneng.2016.06.034

Therefore, it was observed that engine modeling plays an important role while predicting ship performance in rough sea where engine has to operate close to 100% MCR. Whereas, modeling of wake change, thrust and torque losses are important to correctly predict the ship performance in head and bow quartering waves.

7.2.3 The effect of power fluctuation on vessel performance

Engine load variation in presence of waves, including the added resistance has been plotted in Figure 35. In the simulations, propeller emergence was found to occur in head waves of 5m amplitude in cases λ/L=1.1 and 1.6. Due to the propeller emergence, the control system reduces the engine power to control the engine speed as seen in Figure 35. Therefore, in such cases full engine power cannot be utilized causing further drop in speed. Therefore, in Figure 36 the engine load reduces in 5m wave amplitude as compared to 4m wave amplitude for these two cases (λ/L=1.1 and 1.6). This also means that speed prediction in such condition without considering ship motions will predict higher speed. Moreover, having higher engine power will not increase the ship speed in these two cases. Hence, effects like propeller emergence and engine propeller dynamics play an important role in performance prediction of vessel.

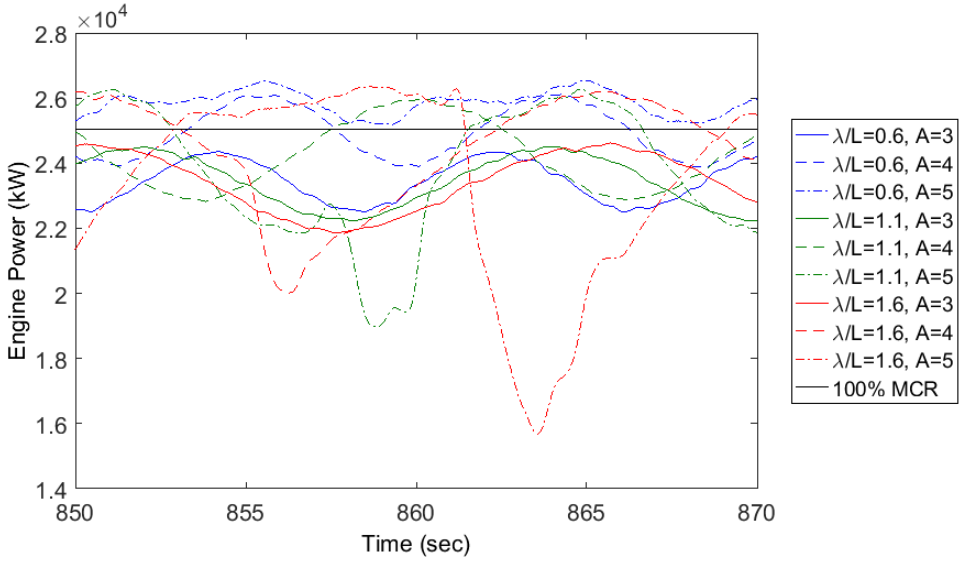

Figure 35 Power variation in waves including added resistance in head waves

DOI: 10.1016/j.oceaneng.2016.06.034

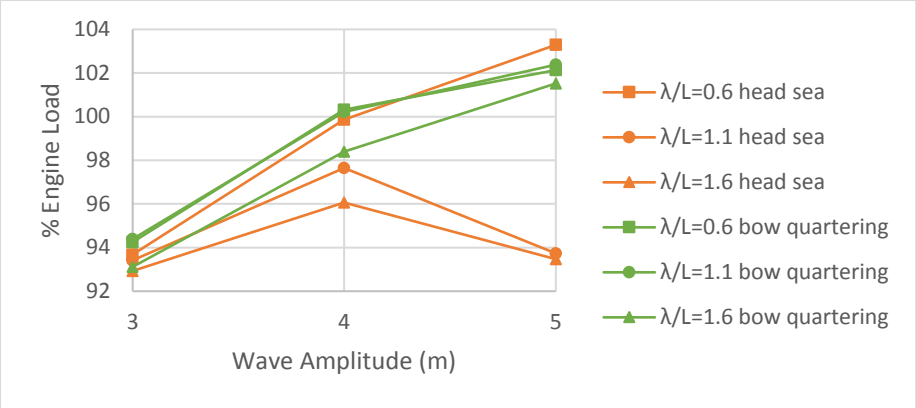

Figure 36 Engine load in presence of head sea and bow quartering waves including the effect of added resistance

Conclusions

In this study, an effective method for modeling wake in waves has been demonstrated which enables us to study different aspects of the propulsion system in time varying wake in waves of different wavelength, waveheight and wave direction. It has been shown that engine propeller response i.e. power fluctuations, propeller speed fluctuations and torque fluctuations can be obtained through coupled simulations by using realistic engine and propeller models. Therefore, the framework of coupled system described in this study can be used to investigate engine load variations, propeller loads in waves, shaft vibration and engine control system. This model is capable of analyzing the performance as well as safety of a control system used for controlling the engine.

Significant changes in the propulsion performance have been observed in presence of waves as compared to steady state operation. Therefore, when estimating the sea margin, drop in propulsion efficiency due to the effect of waves should be taken into account. Engine modeling, wake variation in waves and, thrust and torque losses due to variable propeller submergence are crucial in predicting vessel performance in terms of propulsion efficiency. Wave direction is found to have strong influence on the performance drop, with bow quartering and head sea conditions affecting propulsion performance the most.

Wake variation and engine response will change for different type and sizes of vessels. Hence more vessels should be analyzed in order to draw any generalized conclusions. In this study, an inertial shaft model has been considered. A flexible shaft model can also be implemented in the same framework to study torsional vibrations with realistic engine response and propeller loading. Currently, the analysis has been performed in regular waves. However, in future, simulations can be carried out for irregular wave condition to observe the effect of irregular waves on the overall performance of ship.

Acknowledgements

Authors would like to thank Professor Frederick Stern from the University of Iowa for providing the wake data in waves.

This work is funded by the projects 'Design to Verification of Control Systems for Safe and Energy Efficient Vessels with Hybrid Power Plants' (D2V, NFR: 210670/070), and 'Low Energy and Emission Design of Ships' (LEEDS, NFR 216432/O70) where the Research Council of Norway is the main sponsor of both projects. This work is also supported by the Research Council of Norway through the Centers of Excellence funding scheme, project number 223254 – AMOS.

REFERENCES

Amini, H. (2011). Azimuth propulsors in off-design conditions. Trondheim, Norges teknisk-naturvitenskapelige universitet.

Campora, U. and M. Figari (2003). "Numerical simulation of ship propulsion transients and full-scale validation." Proceedings of the Institution of Mechanical Engineers, Part M: Journal of Engineering for the Maritime Environment **217**(1): 41-52.

Epps, B. (2010). OpenProp v2.4 Theory Document.

Faltinsen, O. M., K. J. Minsaas, N. Liapis and S. O. Skjordal (1980). Prediction of resistance and propulsion of a ship in a seaway. 13th symposium on naval hydrodynamics.

Guo, B. J., S. Steen and G. B. Deng (2012). "Seakeeping prediction of KVLCC2 in head waves with RANS." Applied Ocean Research **35**(0): 56-67.

Hepperle, M. "JavaFoil." from http://www.MH-AeroTools.de/.

Heywood, J. B. (1988). Internal Combustion Engine Fundamentals, McGraw Hill.

Hiroyasu, H., T. Kadota and M. Arai (1983). "Development and use of a spray combustion modeling to predict diesel engine efficiency and pollutant emissions: Part 1 combustion modeling." Bulletin of JSME **26**(214): 569-575.

Incropera, F. P., D. P. DeWitt, T. L. Bergman and A. S. Lavine (2007). Fundamentals of Heat and Mass Transfer, John Wiley & Sons.

ITTC (2008). ITTC – Recommended Procedures and Guidelines. Testing and Extrapolation Methods, Propulsion, Performance, Predicting Powering Margins.

ITTC (2011). Specialist committee on scaling of wake field. Final report and recommendations to the 26th ITTC, ITTC. **Volume 2**.

Kayano, J., H. Yabuki, N. Sasaki and R. Hiwatashi (2013). "A Study on the Propulsion Performance in the Actual Sea by means of Full-scale Experiments." TransNav, the International Journal on Marine Navigation and Safety of Sea Transportation **7**(4): 521-526.

Kyrtatos, N., P. Theodossopoulos, G. Theotokatos and N. Xiros (1999). "Simulation of the overall ship propulsion plant for performance prediction and control." TRANSACTIONS-INSTITUTE OF MARINE ENGINEERS-SERIES C- **111**: 103-114.

Kyrtatos, N. P. (1997). Engine operation in adverse conditions - The ACME project. 2nd international symposium CIMAC. Athens.

Lee, C. S. (1983). Propeller in waves. The 2nd international symposium on practival design in shipbuilding. Tokyo & Seoul.

Livanos, G. A., G. N. Simotas, G. G. Dimopoulos and N. P. Kyrtatos (2006). Simulation of Marine Diesel Engine Propulsion System Dynamics During Extreme Maneuvering. ASME 2006 Internal Combustion Engine Division Spring Technical Conference, American Society of Mechanical Engineers.

DOI: 10.1016/j.oceaneng.2016.06.034

Loukakis, T. A. and P. D. Sclavounos (1978). "Some extensions of the classical approach to strip theory of ship motions, including the calculation of mean added forces and moments." Journal of Ship Research **22**(1): 1-19.

Minsaas, K., O. M. Faltinsen and B. Persson (1983). On the importance of added resistance, propeller immersion and propeller ventilarion for large ships in a seaway. The 2nd international symposium on practical design in shipbuilding. Tokyo & Seoul.

Moor, D. I. and D. C. Murdey (1970). "Motions and Propulsion of Single Screw Models in Head Seas, Part II." The Royal Institution of Naval Architects **Vol. 112**(No. 2).

Nakamura, S. and S. Naito (1975). "Propulsive performance of a container ship in waves." J. Kansai Soc. N. A. Japan **No. 158**.

Queutey, P., J. Wackers, A. Leroyer, G. Deng, E. Guilmineau, G. Hagesteijn and J. Brouwer (2014). Dynamic behaviour of the loads of podded propellers in waves: Experimental and numerical simulations. OMAE2014 San Francisco, California, USA ASME.

Rakopoulos, C. D. and E. Giakoumis (2006). "Review of thermodynamic diesel engine simulations under transient operating conditions." SAE Paper(2006-01): 0884.

Sadat-Hosseini, H., P.-C. Wu, P. M. Carrica, H. Kim, Y. Toda and F. Stern (2013). "CFD verification and validation of added resistance and motions of KVLCC2 with fixed and free surge in short and long head waves." Ocean Engineering **59**(0): 240-273.

Sasajima, H., I. Tanaka and T. Suzuki (1966). "Wake Distribution of Full Ships." Journal of Zosen Kiokai **1966**(120): 1-9.

Sher, E. (1990). "Scavenging the two-stroke engine." Progress in Energy and Combustion Science **16**(2): 95-124.

Takizawa, M., T. Uno, T. Oue and T. Yura (1982). A study of gas exchange process simulation of an automotive multi-cylinder internal combustion engine, SAE Technical Paper.

DOI: 10.1016/j.oceaneng.2016.06.034

Tanizawa, K., Y. Kitagawa, T. Takimoto and Y. Tsukada (2013). "Development of an experimental methodology for self-propulsion test with a marine diesel engine simulator." International Journal of Offshore and Polar Engineering **23**(3): 197-204.

Taskar, B. and S. Steen (2015). Analysis of Propulsion Performance of KVLCC2 in Waves. Fourth International Symposium on Marine Propulsors. Austin, Texas, USA.

Taskar, B., K. K. Yum, E. Pedersen and S. Steen (2015). Dynamics of a marine propulsion system with a diesel engine and a propeller subject to waves. 34th International Conference on Ocean, Offshore and Arctic (OMAE2015). St. John's, Newfoundland, Canada.

Theotokatos, G. and V. Tzelepis (2013). "A computational study on the performance and emission parameters mapping of a ship propulsion system." Proceedings of the Institution of Mechanical Engineers, Part M: Journal of Engineering for the Maritime Environment: 1475090213498715.

Ueno, M., Y. Tsukada and K. Tanizawa (2013). "Estimation and prediction of effective inflow velocity to propeller in waves." Journal of Marine Science and Technology **18**(3): 339-348.

WÄRTSILÄ. (2014). "netGTD Wärtsilä 2-stroke Marine Diesel Engines." Retrieved 12/12, 2014, from http://www.wartsila.com/en/products/netGTD.

Woschni, G. (1967). A universally applicable equation for the instantaneous heat transfer coefficient in the internal combustion engine, SAE Technical paper.

Wu, P. C. (2013). A CFD Study on Added Resistance, Motions and phase averaged wake fields of full form ship model in head waves, Osaka University.

Zacharias, F. (1967). "Analytical Representation of the Thermodynamic Properties of Combustion Gases." SAE Technical Paper **670930**.